What causes southeast Australia's worst droughts?

Caroline C. Ummenhofer,[1] Matthew H. England,[1] Peter C. McIntosh,[2] Gary A. Meyers,[3] Michael J. Pook,[2] James S. Risbey,[2] Alexander Sen Gupta,[1] and Andréa S. Taschetto[1]

Received 26 November 2008; revised 14 January 2009; accepted 22 January 2009; published 24 February 2009.

[1] Since 1995, a large region of Australia has been gripped by the most severe drought in living memory, the so-called "Big Dry". The ramifications for affected regions are dire, with acute water shortages for rural and metropolitan areas, record agricultural losses, the drying-out of two of Australia's major river systems and far-reaching ecosystem damage. Yet the drought's origins have remained elusive. For Southeast Australia, we show here that the "Big Dry" and other iconic 20th Century droughts, including the Federation Drought (1895–1902) and World War II drought (1937–1945), are driven by Indian Ocean variability, not Pacific Ocean conditions as traditionally assumed. Specifically, a conspicuous absence of Indian Ocean temperature conditions conducive to enhanced tropical moisture transport has deprived southeastern Australia of its normal rainfall quota. In the case of the "Big Dry", its unprecedented intensity is also related to recent higher temperatures. **Citation:** Ummenhofer, C. C., M. H. England, P. C. McIntosh, G. A. Meyers, M. J. Pook, J. S. Risbey, A. S. Gupta, and A. S. Taschetto (2009), What causes southeast Australia's worst droughts?, *Geophys. Res. Lett.*, *36*, L04706, doi:10.1029/2008GL036801.

1. Introduction

[2] As the driest inhabited continent on Earth, Australia's climate is harsh and extreme. Rainfall records reveal regular drought cycles, sometimes persisting for a decade and beyond, interspersed with years of above-average rain. The recent multi-year drought gripping southeastern Australia, recently dubbed "The Big Dry", is exceptional [*Sohn*, 2007; *Murphy and Timbal*, 2008] when examined over Australia's climate record of the last 120 years. Drought over eastern Australia has traditionally been linked to the Pacific Ocean with its dominant mode of climate variability, the El Niño-Southern Oscillation (ENSO) [*Nicholls et al.*, 1996; *Power et al.*, 1998]. Here, however, we show, using a suite of observational records that ENSO cannot explain the "Big Dry"; instead, it is predominantly driven by the Indian Ocean Dipole (IOD).

[3] The IOD is a coupled ocean-atmosphere mode of variability in the tropical Indian Ocean characterized by sea surface temperature (SST) anomalies of opposite sign in the east and west, coincident with anomalous large-scale circulation changes around the region [*Saji et al.*, 1999; *Webster et al.*, 1999]. The IOD has widespread effects on rainfall in countries surrounding the tropical Indian Ocean, including East Africa, India and Indonesia [*Webster et al.*, 1999; *Black et al.*, 2003; *Saji and Yamagata*, 2003; *Yamagata et al.*, 2004; *Behera et al.*, 2005, 2006; *D'Arrigo and Smerdon*, 2008]. Over Australia, the effect of the IOD is thought to be primarily limited to western and southern regions of the country [*Ashok et al.*, 2003].

2. Data and Methods

[4] We use monthly data for observed Australian precipitation based on the SILO dataset (1889–2006) [*Jeffrey et al.*, 2001] and observed temperatures from CRUTEM3 (1877–2006) [*Brohan et al.*, 2006]. To investigate the associated climatic conditions during IOD and ENSO events, we also employ the following reanalysis products: HadISST (1877–2006) [*Rayner et al.*, 2003], wind and humidity data from the National Center for Environmental Prediction (NCEP) and the National Center for Atmospheric Research (NCAR) for the period 1948–2006 [*Kalnay et al.*, 1996], and the National Oceanic and Atmospheric Association Palmer Drought Severity Index (PDSI; 1877–2005), which includes the effect of both precipitation and surface air temperatures.

[5] To assess the relative importance of the IOD and ENSO for Southeast Australian drought, all years for the period 1889 to 2006 are classified as to the state of the Indian and Pacific Ocean, respectively (Figure 1a and Table S1 in the auxiliary material).[1] The classification is based on work by *Meyers et al.* [2007], extended to recent years using HadISST data, but retaining the climate shifts defined in the original paper. Of the original 122 years classified, 14 have changed classification. This is not surprising in a method that is not local in time, and that relies on threshold criteria. Results were robust to variations in the thresholds used. The years of importance to this study are the negative IOD years during dry periods, and none of these changed classification.

3. Results

[6] In this study, the region referred to as southeastern Australia is defined as the land region enclosed within 35°–40°S and 140°–148°E (see box in Figure 2f). We assess drought mechanisms over this region during the June–October season, when the majority of the annual precipitation falls. The classification of ENSO and IOD years is shown in Figure 1 (see also Table S1) along with the seasonal mean climate conditions for southeastern Australia

[1]Climate Change Research Centre, University of New South Wales, Sydney, New South Wales, Australia.
[2]Centre for Australian Weather and Climate Research, CSIRO Climate Adaptation Flagship, Hobart, Tasmania, Australia.
[3]Integrated Marine Observing System, University of Tasmania, Hobart, Tasmania, Australia.

0094-8276/09/2008GL036801

[1]Auxiliary materials are available in the HTML. doi:10.1029/2008GL036801.

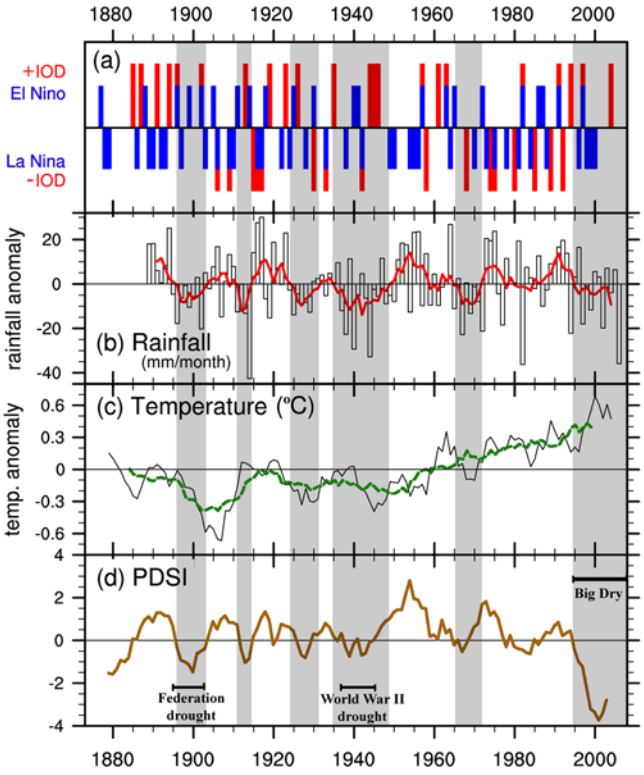

Figure 1. Historical record of IOD and ENSO years and mean climatic conditions over Southeast Australia. (a) Years of positive/negative IOD (red) and El Niño/La Niña (blue) years. (b) Timeseries of anomalous precipitation (mm month^{-1}), with 5-year running mean superimposed in red, (c) 5-yr running mean of temperature (°C), with a 15-year running mean superimposed in green, and (d) 5-yr running mean of Palmer Drought Severity Index (PDSI) over southeastern Australia during June–October. The gray shaded bars highlight periods of below average precipitation when the 5-year running mean falls below one standard deviation. (d) The duration of three major droughts indicated with horizontal black bars.

for the period 1889–2006. An extended period of below-average rainfall is apparent post-1995 (Figure 1b). This period is characterized by severe drought conditions, with the largest negative PDSI value of the 20th Century, close to −4 (Figure 1d). These low-rainfall years are exacerbated by anomalously warm temperatures of 0.3–0.6°C above the long-term average (Figure 1c) [*Cai and Cowan*, 2008a], contributing to the severity of the drought via increased potential evaporation [*Nicholls*, 2004].

[7] Since 1995, several El Niño and positive IOD events have occurred, both generally associated with below-average rainfall across Australia [*Nicholls et al.*, 1996; *Power et al.*, 1998; *Ashok et al.*, 2003; *Saji and Yamagata*, 2003]. However, their frequency (one El Niño and two positive IOD events over 13 years) is not unusual and several periods with substantially more frequent and stronger El Niño or positive IOD events do not exhibit a corresponding multi-year drought. In addition, since it is rare for positive IOD events to evolve successively, they are unlikely to cause multi-year droughts. As a result, it is difficult to argue that the positive IOD and El Niño events are the primary cause of the extreme conditions post-1995. Moreover, four La Niña events have occurred since 1995, which are generally associated with above-average rainfall for the region [*Wang and Hendon*, 2007]. It has been proposed that a reduction in La Niña events contributes to the autumn rainfall decline in Southeast Australia since 1950 [*Cai and Cowan*, 2008b]. However for the Big Dry, with its frequent La Niña events (Figure 1a), this is again unlikely to be a major contributing factor. In contrast, there has been a complete absence of negative IOD events throughout this latest drought period, with the last negative IOD occurring in 1992 (Figure 1a). Negative IOD events are characterized by above-average rainfall over southern regions of Australia resulting from an interaction between the tropics and temperate zone that increases moisture advection onto the region [*Pook et al.*, 2006; *Risbey et al.*, 2009] (see also Figure 2d). This interaction is visible as the often observed northwest cloud-bands [*Tapp and Barrel*, 1984]. The lack of negative IOD events thus deprives Southeast Australia of its normal rainfall quota. In addition, it is apparent from Figure 1c that drought conditions during the Big Dry have been exacerbated by higher temperatures [*Nicholls*, 2004], leading to the lowest PDSI value on record (Figure 1d).

[8] Looking back at the historical record of drought periods in Southeast Australia we find a similar pattern operating for most multi-year droughts throughout the 20th Century. The 1895–1903 Federation Drought for example, which also exhibits very low PDSI values, lies at the end of an extended spell without any negative IOD events (Figure 1). Similarly, the World War II drought (1937–1945) occurred during a period of sustained dry conditions persisting from 1935 to 1949 (Figure 1b), with only one negative IOD event in 1942 (Figure 1a). The rainfall timeseries picks up a modest increase in precipitation during that year, although drought conditions were not broken. The short-lived but intense dry conditions centered around 1913 also occurred in the absence of negative IOD events, exacerbated by several El Niños and a positive IOD event. In the 1920s, anomalous dry conditions persisted from 1924 to 1931, toward the end of a sustained period with no negative IOD events (but three La Niña events) between 1919 and 1930. The anomalous dry years in the late 1960s (1965–1972) again occurred toward the end of an extended period with only one negative IOD and two La Niña events lasting from 1961 to 1972. A consistent feature across the 20th Century southeastern droughts is thus a notable lack of negative IOD events. In contrast, periods with above-average rainfall are often associated with frequent negative IOD events (e.g., 1915–1918, the 1970s and early 1990s; Figures 1a and 1b). Precipitation over Southeast Australia thus seems to be intimately linked to the occurrence of negative IOD events, with all of the main multi-year droughts associated with periods of very few or no events. The net occurrence of only three negative IOD events during the combined multi-year droughts of the past 120 years (highlighted in Figure 1) is highly significant (at the 98% confidence level; as determined by Monte Carlo testing by randomly shuffling the IOD/ENSO categories 10000 times over the period 1889–2006).

[9] To examine the underlying mechanisms linking the IOD and drought conditions, the composited SST, moisture flux (integrated from the surface to 500hPa) and precipita-

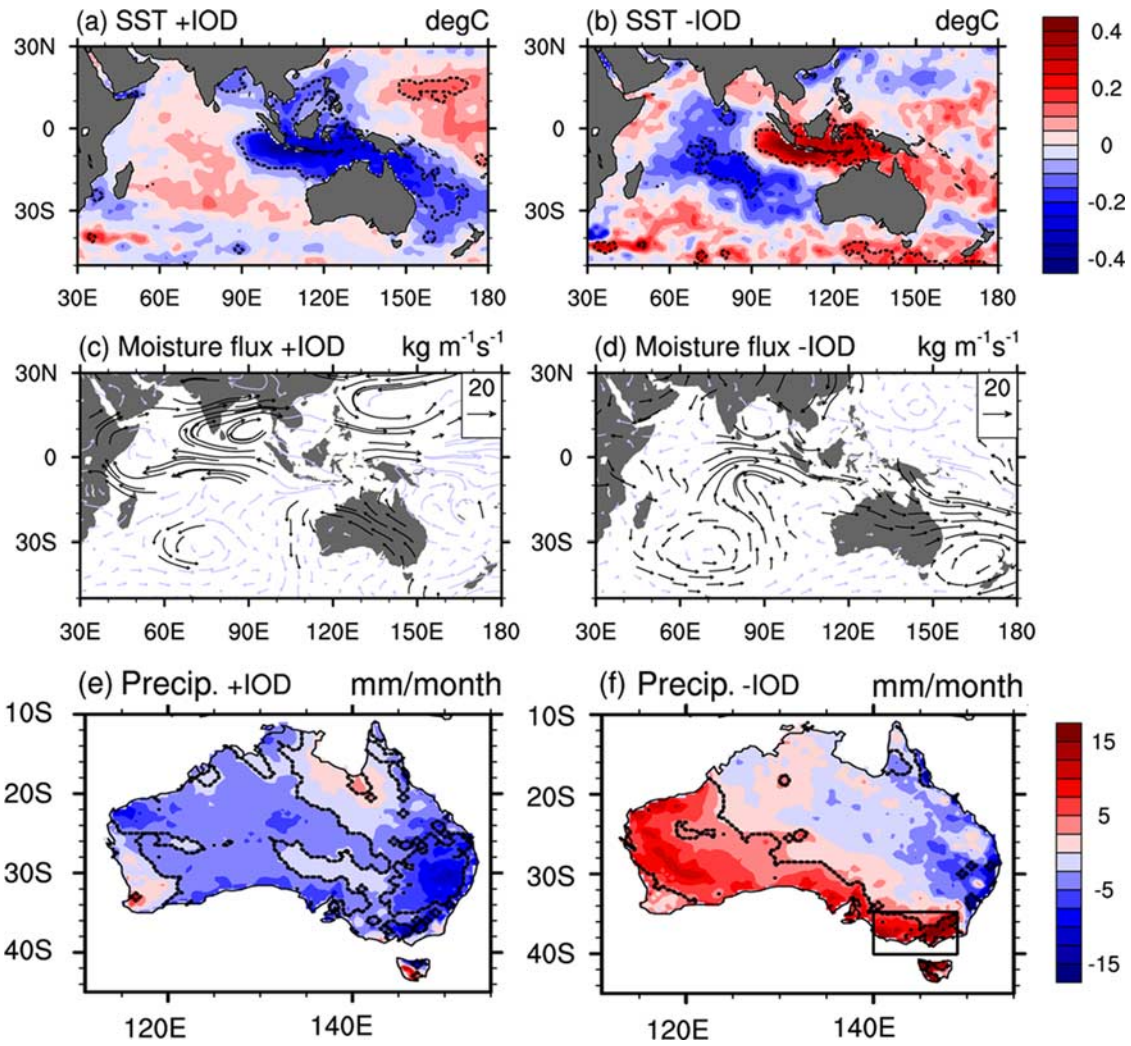

Figure 2. Characteristic climate conditions during pure IOD years. Composite of anomalies in (a, b) SST (°C), (c, d) moisture flux (kg $m^{-1}s^{-1}$), and (e, f) precipitation (mm $month^{-1}$) for the June–October months during pure positive and negative IOD years. The box in Figure 2f indicates the area defined as southeastern Australia for the analyses in Figures 1, 3. Dashed lines and black vectors denote anomalies that are significant at the 80% (90% for SST) confidence level as estimated by a two-tailed *t*-test.

tion during positive and negative IOD events are shown in Figure 2. While still a topic of research, there is increasing evidence that the IOD often occurs independently of ENSO events [*Meyers et al.*, 2007; *Luo et al.*, 2008]. To isolate the effect of the Indian Ocean from ENSO conditions, the composites are only taken for years in which "pure" IOD events occur, i.e. events wherein the state of the Pacific Ocean was neutral with regard to ENSO. The classification presented here uses the longest available record period, but qualitatively similar results are obtained when using other IOD/ENSO classifications [*Yamagata et al.*, 2004].

[10] During positive and negative IOD events, the SST anomaly composites across the Indian Ocean show the characteristic basin-scale dipole pattern (Figures 2a and 2b) [*Saji et al.*, 1999; *Webster et al.*, 1999], with the associated changes to the wind field, leading to changes in moisture flux across the region (Figures 2c and 2d). Moisture flux anomalies during positive IOD events indicate easterly anomalies along the equator in the central and western Indian Ocean (Figure 2c), leading to above-average rainfall over eastern Africa [*Webster et al.*, 1999; *Black et al.*, 2003; *Saji and Yamagata*, 2003; *Ummenhofer et al.*, 2009]. During negative IOD events, in contrast, anomalous eastward moisture flux occurs across the eastern Indian Ocean, bringing enhanced rainfall to the Indonesian Archipelago [*Saji and Yamagata*, 2003]. For Australia, negative IOD events are characterized by enhanced tropical moisture flux reaching southern and western regions (Figure 2d) [*Ansell et al.*, 2000]. The situation is reversed during positive IOD events (Figure 2c). Precipitation anomalies over Australia reveal below-average rainfall for much of the continent during positive IOD events, with anomalies of −10 to −15 mm/month sustained over the east and southeast of the continent (Figure 2e). In contrast, enhanced rainfall is recorded during negative IOD events in Southeast Australia, Tasmania and in the west, with anomalies in the Southeast reaching in excess of 15 mm/month (Figure 2f). An asymmetry is apparent in how positive and negative IOD events

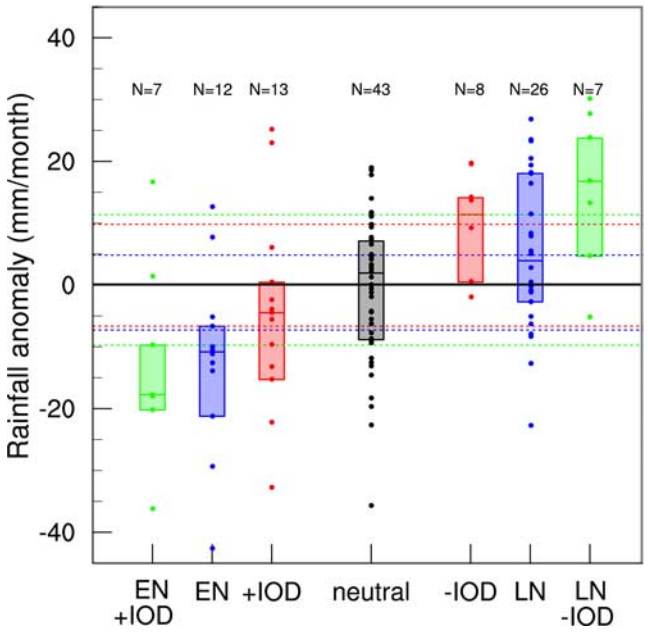

Figure 3. Mean Southeast Australian rainfall anomalies for the different ENSO/IOD categories. June–October rainfall anomalies (mm month^{-1}) over Southeastern Australia shown as dots for pure IOD (red), pure ENSO (blue) and for years with co-occurring ENSO and IOD events (green), with positive events on the left, neutral years (black) in the middle, and negative years on the right. The colored boxes are delimited by the upper and lower quartiles, with the middle bar denoting the median rainfall. Dashed lines indicate the 90% confidence level (as estimated by Monte Carlo testing) for the medians for the different categories (indicated in color), with only the lower (upper) threshold shown for the positive (negative) categories. The number of years (N) in each category is indicated at the top.

project onto precipitation (Figures 2e–2f) over adjacent land-masses around the Indian Ocean. Examining composites of all IOD events, i.e. including those co-occurring with ENSO, previous studies have found that the SST anomalies and associated impacts during the positive phase have a greater magnitude than those during the negative phase. As a result, earlier work has often focused on the positive phase of the IOD [*Black et al.*, 2003; *D'Arrigo and Smerdon*, 2008]. In contrast, here we show that it is actually a lack of the negative IOD phase that provides a more robust explanation for southeastern Australian drought.

[11] To assess the relative importance of ENSO for Southeast Australian climate we also show the composites during "pure" ENSO events, i.e. with the Indian Ocean in a neutral state (Figure S1). The composites reveal the characteristic ENSO pattern of SST anomalies with the El Niño associated with cold temperatures in the western Pacific and warm anomalies across the central and eastern Pacific Ocean. La Niña years exhibit an inverse distribution of temperatures to El Niño. El Niño years are associated with widespread reductions in rainfall across the eastern half of the Australian continent (Figure S1e). During La Niña years, increased onshore moisture flux occurs along the northeast of the country, accounting for the enhanced precipitation over the east and northeast. However, in the southeast of the country, south of 34°S, "pure" La Niña events only show modest above-average rainfall. These anomalous wet conditions are enhanced when looking at all La Niña events, i.e. including those events co-occurring with negative IOD events. Thus, most of the positive impact of La Niña on Southeast Australian rainfall via modulations of the northwest cloudbands described earlier [*Cai and Cowan*, 2008b], may simply be an artifact of the La Niña events co-occurring with a negative IOD phase.

[12] We further explore the relative impact of IOD and ENSO on Southeast Australian precipitation by assessing the regionally-averaged June–October rainfall recorded for individual years in the separate categories; i.e., both pure and combined IOD/ENSO years, as well as for neutral years (Figure 3). Monte Carlo testing was employed to determine the 90% confidence level for the medians to be distinguishable from zero. The median is significantly different from zero in only two of the pure categories, namely during pure El Niño and pure negative IOD years. A median rainfall anomaly of −11 mm/month is recorded for Southeast Australia during pure El Niño years, with all but two events out of twelve showing below-average precipitation. During negative IOD events, the median rainfall anomaly is +12 mm/month, with all but one year out of eight recording above-average precipitation. There is a tendency for positive IOD events to have reduced rainfall and La Niña events to have increased rainfall, but these are not significant at the 90% level. Years with co-occurring ENSO and IOD events record the largest rainfall anomalies over southeastern Australia; in years with both a positive IOD and an El Niño, a median rainfall anomaly of close to −20 mm/month is observed, while a negative IOD co-occurring with La Niña exhibits +16 mm/month above average. To summarize Figure 3, the sign of the rainfall anomalies over Southeast Australia during pure La Niña and positive IOD events is highly variable, whereas El Niño years consistently result in dry conditions and negative IOD years consistently in wet conditions (see also Figure S1). Moreover, a lack of negative IOD events is observed throughout most of the multi-year droughts of the 20th Century, and in particular is a prominent feature of the present Big Dry (Figure 1). The same cannot be said about ENSO, with both negative and positive phases occurring during all of the major 20th Century droughts.

4. Conclusion

[13] We have demonstrated that Indian Ocean variability, more than ENSO, is the key driver of the major droughts over the past 120 years in the region of southeastern Australia examined in this study. In particular during virtually all of Australia's iconic droughts, including the Federation Drought (1895–1902), the World War II drought (1937–1945), and the present "Big Dry" (post-1995), the IOD has remained persistently 'positive' or 'neutral'. During the negative phase of the IOD, unusually wet conditions dominate across southern regions of Australia, due to an interaction between the tropics and the temperate zone that increases regional moisture advection. The conspicuous lack of the "negative" phase of the IOD during the major droughts thus deprives Southeast Australia of its normal rainfall quota. Future work will use climate model output to

test the robustness of our main findings. Despite the prominent role of the Indian Ocean in driving southeastern droughts, the severity of the "Big Dry" is still exceptional; this appears to be linked to recent large increases in air temperature.

[14] IOD events may be predictable out to several months in advance [*Luo et al.*, 2008]. Exploitation of this predictability could therefore lead to significant improvements in water planning and agricultural management in a drought-stricken region. This heightens the need for improved and sustained Indian Ocean observations. Recent non-uniform warming trends in the Indian Ocean [*Ihara et al.*, 2008] raise the possibility that the characteristics of positive and negative IOD events might be changing. Modifications to the frequency and decadal cycles in the IOD could result in major impacts for Indian Ocean rim nations.

[15] **Acknowledgments.** The NCEP/NCAR reanalysis and PDSI were provided by NOAA/OAR/ESRL PSD, USA, HadISST by the UK Met Office, CRUTEM3 by the Climate Research Unit, University of East Anglia, UK, and the SILO data is from the Australian Bureau of Meteorology. John Church, Ben McNeil, and two anonymous reviewers provided helpful comments on the manuscript. C.C.U., M.H.E., A.S.G. and A.S.T. were supported by the Australian Research Council.

References

Ansell, T. J., C. J. C. Reason, I. N. Smith, and K. Keay (2000), Evidence for decadal variability in southern Australian rainfall and relationships with regional pressure and sea surface temperature, *Int. J. Climatol.*, *20*, 1113–1129.

Ashok, K., Z. Guan, and T. Yamagata (2003), Influence of the Indian Ocean dipole on the Australian winter rainfall, *Geophys. Res. Lett.*, *30*(15), 1821, doi:10.1029/2003GL017926.

Behera, S. K., J.-J. Luo, S. Masson, P. Delecluse, S. Gualdi, A. Navarra, and T. Yamagata (2005), Paramount impact of the Indian Ocean dipole on the East African short rains: A CGCM study, *J. Clim.*, *18*, 4514–4530.

Behera, S. K., J.-J. Luo, S. Masson, S. A. Rao, H. Sakuma, and T. Yamagata (2006), A CGCM study on the interaction between IOD and ENSO, *J. Clim.*, *19*, 1688–1705.

Black, E., J. Slingo, and K. R. Sperber (2003), An observational study of the relationship between excessively strong short rains in coastal East Africa and Indian Ocean SST, *Mon. Weather Rev.*, *131*, 74–94.

Brohan, P., J. J. Kennedy, I. Harris, S. F. B. Tett, and P. D. Jones (2006), Uncertainty estimates in regional and global observed temperature changes: A new data set from 1850, *J. Geophys. Res.*, *111*, D12106, doi:10.1029/2005JD006548.

Cai, W., and T. Cowan (2008a), Evidence of impacts from rising temperature on inflows to the Murray-Darling Basin, *Geophys. Res. Lett.*, *35*, L07701, doi:10.1029/2008GL033390.

Cai, W., and T. Cowan (2008b), Dynamics of late autumn rainfall reduction over southeastern Australia, *Geophys. Res. Lett.*, *35*, L09708, doi:10.1029/2008GL033727.

D'Arrigo, R., and J. E. Smerdon (2008), Tropical climate influences on drought variability over Java, Indonesia, *Geophys. Res. Lett.*, *35*, L05707, doi:10.1029/2007GL032589.

Ihara, C., Y. Kushnir, and M. A. Cane (2008), Warming trend of the Indian Ocean SST and Indian Ocean dipole from 1880 to 2004, *J. Clim.*, *21*, 2035–2046.

Jeffrey, S. J., J. O. Carter, K. B. Moodie, and A. R. Beswick (2001), Using spatial interpolation to construct a comprehensive archive of Australian climate data, *Environ. Modell. Software*, *16*, 309–330.

Kalnay, E., et al. (1996), The NCEP/NCAR 40-year reanalysis project, *Bull. Am. Meteorol. Soc.*, *77*, 437–471.

Luo, J.-J., S. Behera, Y. Masumoto, H. Sakuma, and T. Yamagata (2008), Successful prediction of the consecutive IOD in 2006 and 2007, *Geophys. Res. Lett.*, *35*, L14S02, doi:10.1029/2007GL032793.

Meyers, G., P. McIntosh, L. Pigot, and M. Pook (2007), The years of El Niño, La Niña and interactions with the tropical Indian Ocean, *J. Clim.*, *20*, 2872–2880.

Murphy, B. F., and B. Timbal (2008), A review of recent climate variability and climate change in southeastern Australia, *Int. J. Climatol.*, *28*, 859–879.

Nicholls, N. (2004), The changing nature of Australian droughts, *Clim. Change*, *63*, 323–336.

Nicholls, N., B. Lavery, C. Frederiksen, and W. Drosdowsky (1996), Recent apparent changes in relationships between the El Niño–Southern Oscillation and Australian rainfall and temperature, *Geophys. Res. Lett.*, *23*, 3357–3360.

Pook, M. J., P. C. McIntosh, and G. A. Meyers (2006), The synoptic decomposition of cool season rainfall in the southeastern Australian cropping region, *J. Appl. Meteorol. Clim.*, *45*, 1156–1170.

Power, S., F. Tseitkin, S. Torok, B. Lavery, R. Dahni, and B. McAvaney (1998), Australian temperature, Australian rainfall and the Southern Oscillation, 1910–1992: Coherent variability and recent changes, *Aust. Meteorol. Mag.*, *47*, 85–101.

Rayner, N. A., D. E. Parker, E. B. Horton, C. K. Folland, L. V. Alexander, D. P. Rowell, E. C. Kent, and A. Kaplan (2003), Global analyses of sea surface temperature, sea ice, and night marine air temperature since the late nineteenth century, *J. Geophys. Res.*, *108*(D14), 4407, doi:10.1029/2002JD002670.

Risbey, J. S., M. J. Pook, P. C. McIntosh, C. C. Ummenhofer, and G. A. Meyers (2009), Variability of synoptic features associated with cool season rainfall in southeastern Australia, *Int. J. Climatol.*, in press.

Saji, H. N., and T. Yamagata (2003), Possible impacts of Indian Ocean dipole mode events on global climate, *Clim. Res.*, *25*, 151–169.

Saji, N. H., B. N. Goswami, P. N. Vinayachandran, and T. Yamagata (1999), A dipole mode in the tropical Indian Ocean, *Nature*, *401*, 360–363.

Sohn, E. (2007), The Big Dry, *Sci., News*, *172*, 17.

Tapp, R. G., and S. L. Barrel (1984), The north-west Australian cloud band: Climatology, characteristics and factors associated with development, *Int. J. Climatol.*, *4*, 411–424.

Ummenhofer, C. C., A. Sen Gupta, M. H. England, and C. J. C. Reason (2009), Contributions of Indian Ocean sea surface temperatures to enhanced East African rainfall, *J. Clim.*, vol. 22, No 4, p. 993–1013.

Wang, G., and H. Hendon (2007), Sensitivity of Australian rainfall to inter–El Niño variations, *J. Clim.*, *20*, 4211–4226.

Webster, P. J., A. M. Moore, J. P. Loschnigg, and R. R. Leben (1999), Coupled ocean-atmosphere dynamics in the Indian Ocean during 1997–98, *Nature*, *401*, 356–360.

Yamagata, T., S. Behera, J.-J. Luo, S. Masson, M. R. Jury, and S. A. Rao (2004), Coupled ocean-atmosphere variability in the tropical Indian Ocean, in *Earth's Climate: The Ocean-Atmosphere Interaction*, *Geophys. Monogr. Ser.*, vol. 147, edited by C. Wang, S.-P. Xie, and J. Carton, pp. 189–211, AGU, Washington, D. C.

M. H. England, A. S. Gupta, A. S. Taschetto, and C. C. Ummenhofer, Climate Change Research Centre, University of New South Wales, Sydney, NSW 2052, Australia. (c.ummenhofer@unsw.edu.au)

P. C. McIntosh, M. J. Pook, and J. S. Risbey, Centre for Australian Weather and Climate Research, CSIRO Climate Adaptation Flagship, GPO Box 1538, Hobart, TAS 7001, Australia.

G. A. Meyers, Integrated Marine Observing System, University of Tasmania, Hobart, TAS 7001, Australia.